

Forschungszentrum Karlsruhe
Technik und Umwelt

Wissenschaftliche Berichte
FZKA 6067

42077

Corrosion Evaluation of Metallic Materials for Long-Lived HLW/Spent Fuel Disposal Containers

**E. Smailos, A. Martinez-Esparza,
B. Kursten, G. Marx, I. Azkarate**
Institut für Nukleare Entsorgungstechnik

Februar 1998

FORSCHUNGSZENTRUM KARLSRUHE

Technik und Umwelt

Wissenschaftliche Berichte

FZKA 6067

**Corrosion Evaluation of Metallic Materials for
Long-Lived HLW/Spent Fuel Disposal Containers**

**E. Smailos, A. Martínez-Esparza¹⁾, B. Kursten²⁾, G. Marx³⁾,
I. Azkarate⁴⁾**

Institut für Nukleare Entsorgungstechnik

¹⁾ ENRESA, Madrid (E), ²⁾ SCK.CEN, Mol (B), ³⁾ FU Berlin (D),
⁴⁾ INASMET, San Sebastian (E)

EC-Contract No. FI4W-CT95-0002

Annual Progress Report 1997

Forschungszentrum Karlsruhe GmbH, Karlsruhe
1998

Als Manuskript gedruckt
Für diesen Bericht behalten wir uns alle Rechte vor

Forschungszentrum Karlsruhe GmbH
Postfach 3640, 76021 Karlsruhe

Mitglied der Hermann von Helmholtz-Gemeinschaft
Deutscher Forschungszentren (HGF)

ISSN 0947-8620

SUMMARY

The investigations into the influence of important parameters on the corrosion behaviour of preselected container materials (carbon steel, Cr-Ni steels, Hastelloy C4 and Ti99.8-Pd) in salt, granite and clay environments have been continued. Parameters investigated were: temperature (16°C–170°C), pH (1–10), selected chemical species (Cl^- , SO_4^{2-} , $\text{S}_2\text{O}_3^{2-}$, $\text{B}(\text{OH})_4^-$, Fe^{3+} , H_2O_2 , ClO^- , F^-), and strain rates of $10^{-4} - 10^{-7} \text{ s}^{-1}$.

Present results obtained in NaCl-rich brine (170°C) indicate that initial pH values of 1–5 do not influence significantly the corrosion rate of the TStE355 carbon steel (42–50 $\mu\text{m/a}$). Higher pH values (6–10) decrease the corrosion rate of the steel (26–28 $\mu\text{m/a}$). Chemical species such as $\text{B}(\text{OH})_4^-$ and Fe^{3+} accelerate the corrosion rate of the steel in the brine at 90°C and 170°C. According to the electrochemical studies on Ti99.8-Pd, realistic concentrations of H_2O_2 (10^{-4} – 10^{-5} mol/l), ClO^- (10^{-1} mol/l) and F^- (10^{-1} – 10^{-3} mol/l) in repository brines do not enhance the corrosion rate of this alloy in the temperature range of 25°C–80°C.

In synthetic bentonite granitic water ($T = 90^\circ\text{C}$) and very slow strain rates, the TStE355 steel is not sensitive to stress corrosion cracking. However, it exhibits a loss of ductility which is attributed to hydrogen embrittlement. In oxidizing clay water, the resistance of the materials to pitting corrosion decreases with increasing temperature and Cl^- content. On the contrary, the resistance to pitting corrosion increases with increasing SO_4^{2-} content. The influence of $\text{S}_2\text{O}_3^{2-}$ to pitting corrosion of the materials in clay water depends on the material type. Among the materials investigated, Hastelloy C4 exhibits the highest resistance to pitting corrosion in oxidizing clay water.

Bewertung von metallischen Werkstoffen für langzeitbeständige HAW-Endlagerbehälter im Hinblick auf ihre Korrosionsbeständigkeit

Zusammenfassung

Die Untersuchungen zum Einfluß wichtiger Parameter auf das Korrosionsverhalten ausgewählter Behältermaterialien (unlegierter Stahl, Cr-Ni-Stähle, Hastelloy C4 und Ti99.8-Pd) unter Endlagerbedingungen in Steinsalz, Granit und Ton wurden fortgeführt. Untersuchte Parameter waren: Temperatur (16°C-170°C), pH (1-10), ausgewählte chemische Spezies (Cl^- , SO_4^{2-} , $\text{S}_2\text{O}_3^{2-}$, $\text{B}(\text{OH})_4^-$, Fe^{3+} , H_2O_2 , ClO^- , F^-) und langsame Dehnungsraten von 10^{-4} - 10^{-7} s^{-1} .

Die Ergebnisse in NaCl-reicher Lösung (170°C) zeigen, daß anfängliche pH-Werte von 1-5 keinen signifikanten Einfluß auf die Korrosionsrate des Feinkornbaustahls TStE355 haben (42-50µm/a). Höhere pH-Werte (6-10) erniedrigen die Korrosionsrate des Stahls (26-28µm/a). Chemische Spezies wie $\text{B}(\text{OH})_4^-$ und Fe^{3+} erhöhen die Korrosionsrate des Stahls in der Lösung bei 90°C und 170°C. Die Ergebnisse elektrochemischer Untersuchungen an Ti99.8-Pd (T=25°C-80°C) zeigen, daß realistische Konzentrationen von H_2O_2 (10^{-4} - 10^{-5} mol/l), ClO^- (10^{-1} mol/l) und F^- (10^{-1} - 10^{-3} mol/l) in Endlagersalzlösungen zu keiner Erhöhung der Korrosionsrate führen.

In Granitwasser bei 90°C und sehr langsamen Dehnungsraten ist der Stahl TStE355 beständig gegenüber Spannungsrißkorrosion, jedoch nimmt seine Duktilität ab, was auf den versprödenden Effekt des Korrosionswasserstoffs zurückgeführt wird. In oxidierendem Tonwasser (T=16°C-90°C) nimmt die Lochkorrosionsbeständigkeit der Werkstoffe mit steigender Temperatur und Cl^- -Gehalt ab. Im Gegensatz dazu ist die Lochkorrosionsbeständigkeit der Werkstoffe um so höher, je größer die SO_4^{2-} -Konzentration im Tonwasser ist. Der Einfluß von $\text{S}_2\text{O}_3^{2-}$ auf die Korrosion hängt vom Werkstoff ab. Von allen untersuchten Werkstoffen zeigt Hastelloy C4 die höchste Korrosionsresistenz gegenüber oxidierendem Tonwasser.

TABLE OF CONTENTS

	Page
Summary	
A. Objectives and scope	1
B. Work programme	1
C. Progress of work and results obtained	2
C.1 Corrosion studies on candidate container materials in salt environments	2
C.1.1 Long-term immersion tests (FZK.INE)	2
C.1.2 Electrochemical and radiochemical studies (FU Berlin)	6
C.1.3 Stress corrosion cracking studies in salt and granite environments (ENRESA/INASMET)	12
C.2 Corrosion studies on candidate container materials in clay/bentonite environments (SCK.CEN)	15
D. Conclusions	18
E. Planned work for the next reporting period	19
F. References	20

10/10/10

10/10/10

10/10/10

10/10/10

10/10/10

10/10/10

10/10/10

10/10/10

10/10/10

10/10/10

10/10/10

10/10/10

10/10/10

10/10/10

10/10/10

10/10/10

10/10/10

10/10/10

10/10/10

10/10/10

10/10/10

10/10/10

10/10/10

10/10/10

10/10/10

10/10/10

10/10/10

10/10/10

A. OBJECTIVES AND SCOPE

In previous corrosion studies [1,2,3], two approaches were identified for the manufacture of long-lived HLW/Spent Fuel disposal containers that could act as a radionuclide barrier in repositories in rock salt, granite and clay. These are the corrosion allowance concept and the corrosion-resistant concept. For corrosion-allowance, carbon steels are the most promising material for all three rock formations. For corrosion-resistant, the strongest candidates are the alloy Ti99.8-Pd (Ti/0.2 Pd, TiGr-7) for rock salt, and stainless steels for granite and clay.

In the present research programme, further in-depth corrosion studies will be performed on the abovementioned materials in rock salt, granite and clay environments. These include: long-term immersion tests, electrochemical/radiochemical studies and slow strain rate tests. The objectives of the studies are:

- to investigate the potential effect of essential parameters on corrosion.
- to gain a better understanding of corrosion mechanisms.
- to provide more accurate data for a material degradation model that can be used to predict the lifetime of such containers.

B. WORK PROGRAMME

B.1 Corrosion studies on candidate container materials in salt environments

1.1 Long-term immersion tests are performed on the TStE355 carbon steel (0.17 wt.% C) and Ti99.8-Pd in salt brines aimed at evaluating the effect of essential parameters on their corrosion behaviour. Such parameters are: the pH of the brines, the content of salt impurities, gamma-radiation, and welding (FZK.INE).

1.2 Combined electrochemical and radiochemical studies are performed on Ti99.8-Pd in salt brines in order to get a detailed insight into corrosion kinetics and especially into the potential influence of the radiolytic product H_2O_2 on corrosion. Both unwelded and welded specimens are examined (FU Berlin).

1.3 The resistance of Ti99.8-Pd (TiGr-7) and TStE355 carbon steel (0.17 wt.% C) to stress corrosion cracking (SCC) is investigated in an NaCl brine (25.9 wt.% NaCl)

at 170°C and strain rates of 10^{-4} - 10^{-7} s⁻¹ by means of the slow strain rate technique (SSRT). For comparison, additional investigations are conducted in argon as inert reference medium (ENRESA/INASMET).

B.2 Stress corrosion cracking studies in granite environments

The resistance of the AISI 316L stainless steel and TStE355 carbon steel to stress corrosion cracking (SCC) in a bentonite buffered granitic groundwater is investigated at 90°C at various slow strain rates (ENRESA/INASMET).

B.3 Corrosion studies in clay/bentonite environments

Electrochemical corrosion studies are performed on candidate container materials aimed at investigating the influence of important environmental parameters on corrosion. Such parameters are: the temperature (16°C and 90°C), and the content of O₂, Cl⁻, SO₄²⁻ and S₂O₃²⁻ of the corrosion medium (SCK.CEN).

C. PROGRESS OF WORK AND RESULTS OBTAINED

C.1 Corrosion studies on candidate container materials in salt environments (Work Package 1)

C.1.1 Long-term immersion tests (FZK.INE)

Long-term immersion tests are performed on the TStE355 carbon steel (0.17 wt.% C) and Ti99.8-Pd in salt brines aimed at evaluating the effect of essential parameters on their corrosion behaviour. Such parameters are: the pH of the brines, the content of salt impurities, gamma radiation, and welding.

In the period under review, the investigations into the influence of pH on the corrosion of the TStE355 carbon steel in salt brines were continued and concluded. Furthermore, the effect of selected chemical species present in the bulk brine environment on the corrosion of the steel was examined at higher temperatures.

Influence of pH on the corrosion of TStE355 carbon steel in NaCl-rich brine

In addition to previous investigations in the MgCl₂-rich „Q-brine“ [4], the effect of pH values between 1 and 10 on the corrosion of the TStE355 carbon steel was examined in an NaCl-rich brine (brine M3) at the disposal-relevant temperature of 170°C. The steel was tested in the hot-rolled and annealed condition. For the investigations plane specimens having the dimensions 40mmx20mmx3-4mm were used. The steel had the following composition in wt. %:

0.17 C; 0.44 Si; 1.49 Mn; bal. Fe.

The composition of the corrosion medium (brine M3) was (wt.% at 55°C) :

25.9 NaCl; 0.23 K₂SO₄; 0.21 CaSO₄; 0.16 MgSO₄; 73.5 H₂O (pH (21°C) = 6.0)

The various pH values were adjusted by addition of HCl or NaOH to the brine. The experiments lasted up to 1 year. The experimental setup is described elsewhere [5]. Shortly, for the experiments stainless steel pressure vessels with corrosion resistant PTFE inserts were used. After tightly closing the inserts, the vessels were stored in heated chambers at the 170°C test temperature. After removal from the brines, the specimens were examined for general and pitting corrosion by gravimetry, pitting measurements, surface profilometry and metallography.

The results indicate that the steel is resistant to pitting corrosion at all pH values of the brine. A slight non-uniform general corrosion was observed, and the thickness reduction of the specimens increased linearly with the corrosion time. Figures 1 and 2 show by way of example optical micrographs of steel specimens after 1 year exposure to the brine at pH values of 1 and 10. The linear time-dependence of the thickness reduction of the steel in the brine at 170°C and pH = 1 is shown in Figure 3. Figure 4 shows the integral corrosion rate of the steel in dependence of the initial pH values of the brine. In the range between 1 and 5, the pH has no significant influence on the corrosion rate. The values (42 μm/a - 50 μm/a) differ among one another only about 20% at the maximum which is within the statistical variations of the measured values. With increase of the pH from 5 to 6, the corrosion rate of the steel clearly decreases to 28 μm/a. A further increase of the pH, however, does not practically change the corrosion rate (26 μm/a at pH = 10). It is important to mention

that after termination of the exposure time, nearly the same pH value of 5.4 - 5.7 was measured in all brines independent of their initial pH. It appears that the pH of the brine will be buffered by the reaction of corrosion products with brine constituents. This is probably the reason that initial pH values of the brine between 1 and 5 have no significant influence on steel corrosion. The lower corrosion rates at the higher pH values of 6 to 10 may be explained by the formation of a very dense corrosion protection layer which was observed after termination of the experiments.

Effect of chemical species on the corrosion of TStE355 carbon steel in NaCl-rich brine

An important aspect of the corrosion studies is the investigation of the influence of chemical species present in the bulk brine environment on the corrosion of the TStE355 steel. Such species may intrude into the brines, e. g. as salt impurities or be generated by gamma radiolysis of the brines, and can significantly affect the corrosion behaviour of the steel by various processes (e. g. change of redox potential, formation of complexes). Therefore, long-term corrosion studies (immersion tests) were performed to evaluate the effect of some selected salt impurities and gamma radiolytic products on the corrosion of the steel in an NaCl-rich brine (brine M3, composition as given above).

Following species were added to the brine: the salt impurity B(OH)_4^- , the main gamma radiolytic products of the brine H_2O_2 and ClO^- , and F^{3+} . The latter can be generated by oxidation of the container corrosion product Fe^{2+} as a result of radiolysis or ingress of oxygen into the disposal area. The concentration of the various species in the brine varied between 10^{-1} mol/l and 10^{-3} mol/l (Table I). Both the individual and the synergistic effect of the chemical species on the steel corrosion was investigated up to 520 days in the brine at 90°C and 170°C . For this, the species were added to the brine single and all simultaneously, respectively. For comparison, investigations were performed in the NaCl-rich brine also without addition of chemical species („pure brine“). The experimental setup used and the post-examination methods applied for evaluation of the specimens for corrosion

attacks are described before (page 3).

The results indicate that in all brines with and without additions of chemical species, the thickness reduction of the steel specimens (general corrosion) increases linearly with the exposure time. The integral corrosion rate of the steel over a test period of up to 520 days in the various brines is very small ($5 \mu\text{m/a}$). The addition of the chemical species to the brine (single or all species simultaneously) significantly increases the corrosion rate of the steel. The highest rates occur in the brines containing B(OH)_4^- ($102 \mu\text{m/a}$) and all species simultaneously ($236 \mu\text{m/a}$). The latter indicates a synergistic effect.

At 170°C the corrosion rate in the pure brine ($46 \mu\text{m/a}$) is clearly higher than at 90°C ($5 \mu\text{m/a}$). However, the addition of the chemical species to the brine does not significantly increase the corrosion rate of the steel over the value in the pure brine. The maximum corrosion rates at 170°C occur in the brines containing B(OH)_4^- ($58 \mu\text{m/a}$), Fe^{3+} ($59 \mu\text{m/a}$) and all species simultaneously ($73 \mu\text{m/a}$). These values are only a factor 1.3 - 1.6 higher than those in the pure brine.

The comparison of the results obtained at the two test temperatures shows that the increase of the temperature from 90°C to 170°C accelerates the corrosion rates of the steel only in the pure brine, and to a certain extent in the ClO^- -containing brine. In fact, in the brines containing B(OH)_4^- , Fe^{3+} and all species, respectively, the corrosion rates at 170°C are lower than at 90°C . This is attributed to the formation of a very dense corrosion protection layer at 170°C which was observed in the metallographic examinations. However, after long exposure times, the corrosion layer formed in the brine containing all species broke down locally, and a non-uniform corrosion with a maximum penetration depth of $130 \mu\text{m}$ was observed after 1 year exposure time. In all other brines at both test temperatures, the corrosion of the steel was nearly uniform.

C.1.2 Electrochemical and radiochemical studies (FU Berlin)

Combined electrochemical and radiochemical studies are performed on Ti99.8-Pd in salt brines in order to get a detailed insight into the corrosion kinetics and especially into the potential influence of the radiolytic products H_2O_2 and ClO^- on corrosion. Both unwelded and welded specimens are examined. The studies are performed in MgCl_2 -rich brine (Q-brine) and in two NaCl brines at temperatures between 25°C and 80°C at Free Corrosion Potential (E_{corr}) and at various applied potentials. The method used is the Radioisotope Method (RIM) which combines classical electrochemical procedures (potentiostatic and potentiodynamic measurements, impedance and photocurrent measurements) with radiochemical ones, especially neutron activation analysis. Furthermore, microscopic examinations are carried out in order to decide whether pit corrosion or general corrosion has taken place.

In the period under review, work has been concentrated above all on the investigation of the influence of H_2O_2 on corrosion of Ti99.8-Pd in the three above-mentioned solutions at various temperatures. Both unwelded (parent material) and TIG-welded Ti99.8-Pd were examined. For a better understanding of the results obtained in the H_2O_2 containing solutions, corresponding corrosion studies were performed in solutions containing F^- . In addition to these studies, the effect of the other radiolytic product ClO^- on the corrosion of Ti99.8-Pd was investigated.

Influence of H_2O_2 on the corrosion of Ti99.8-Pd

The effect of H_2O_2 on the corrosion of Ti99.8-Pd was studied in three brines at rest potential and various applied potentials at temperatures of 25°C - 80°C. The initial concentration of H_2O_2 in the brines ranged from $7 \cdot 10^{-5}$ mol/l to $1.4 \cdot 10^{-1}$ mol/l. The brines used had the following composition (wt. %):

Saturated NaCl brine: 26.9 NaCl; 73.1 H_2O .

NaCl-rich brine (brine 3): 25.9 NaCl; 0.23 K_2SO_4 ; 0.21 CaSO_4 ; 0.16 MgSO_4 ; 73.5 H_2O .

Q-brine (MgCl_2 -rich): 26.8 MgCl_2 ; 4.7 KCl; 1.4 MgSO_4 ; 1.4 NaCl; 65.7 H_2O .

General kinetical calculations for H₂O₂

The H₂O₂ concentration in the solutions changes with time. Therefore, during the experiments the H₂O₂ content was measured by use of iodometric titration. The following logarithmic relationship was found between H₂O₂ concentration $c_{\text{H}_2\text{O}_2}$ and time t :

$$c_{\text{H}_2\text{O}_2} = c_{\text{H}_2\text{O}_2}^0 \cdot e^{-k_3 \cdot t} \quad (1)$$

Here $c_{\text{H}_2\text{O}_2}^0$ is the initial concentration and k_3 is the velocity constant of the H₂O₂ decay. At 25°C k_3 is found to be $(3 \pm 1) \cdot 10^{-2} \text{h}^{-1}$. Therefore, an average H₂O₂ concentration can be calculated.

The evaluation of the time dependence of the mass loss determined by γ -spectroscopy makes the titanium corrosion under the influence of H₂O₂ be described kinetically.

The change of the titanium concentration vs time is given by equation (2):

$$\left(\frac{dc_{\text{Ti;Sol}}}{dt} \right) = k_1' + k_2' \cdot c_{\text{H}_2\text{O}_2} \quad (2)$$

Here k_1' is the velocity constant of corrosion in a solution, being free of H₂O₂, and k_2' is the velocity constant of corrosion in the presence of H₂O₂.

Under experimental conditions the peroxide concentration $c_{\text{H}_2\text{O}_2}$ is not constant and equation (1) must be taken into consideration. In this case, the amount of the dissolved titanium $c_{\text{Ti; sol}}$ can be calculated from equation (3) for every time:

$$c_{\text{Ti;Sol}} = k_1' \cdot t + \frac{k_2' \cdot c_{\text{H}_2\text{O}_2}^0}{k_3} \cdot (1 - e^{-k_3 \cdot t}) \quad (3)$$

For a known constant H₂O₂ concentration the corrosion rate w is given by equation (4).

$$w = \left(\frac{dc_{\text{Ti;Sol}}}{dt} \right) \cdot \frac{V_{\text{Sol}} \cdot M_{\text{Ti}}}{A_{\text{EI}} \cdot \rho_{\text{Ti}}} = (k_1' + k_2' \cdot c_{\text{H}_2\text{O}_2}) \cdot \frac{V_{\text{Sol}} \cdot M_{\text{Ti}}}{A_{\text{EI}} \cdot \rho_{\text{Ti}}} \quad (4)$$

Here V_{Sol} is the volume of the solution, M_{Ti} the molar mass of titanium, A_{El} the area of the electrode and r_{Ti} the density of titanium.

For a variable H_2O_2 concentration, $c_{\text{H}_2\text{O}_2}$ is given by equation (1).

In saturated NaCl solution at 25°C the velocity constants are: $k_1' = (9 \pm 8) \cdot 10^{-10} \text{ mol/l} \cdot \text{h}$ and $k_2' = (16 \pm 5) \cdot 10^{-7} \text{ h}^{-1}$.

Kinetical calculations for H_2O_2 under practical conditions

Under practical conditions in a waste repository the H_2O_2 concentration is in equilibrium. That means the rate of radiolytical H_2O_2 production equals the rate of H_2O_2 decay:

$$\left(+ \frac{dc_{\text{H}_2\text{O}_2}}{dt} \right)_{\text{prod.}} = \left(- \frac{dc_{\text{H}_2\text{O}_2}}{dt} \right)_{\text{desint.}} = k_3 \cdot c_{\text{H}_2\text{O}_2; \text{eq}} \quad (5)$$

Taking equation (6) into account [6]

$$G = \frac{c_{\text{H}_2\text{O}_2} \cdot N_A}{D_a \cdot \rho_{\text{Sol}}} \quad (6)$$

the H_2O_2 concentration can be calculated with the following equation:

$$c_{\text{H}_2\text{O}_2} = \frac{G \cdot \dot{D}_a^{\text{max}} \cdot \rho_{\text{Sol}}}{k_3 \cdot N_A} \quad (7)$$

Here G is 0.70 per 100 eV and the permitted dose rate \dot{D}_a^{max} is 0.2 mGy/h. The density of the relevant salt solution r_{Sol} is 1.2 g/cm^3 , the velocity constant of peroxide decay is $(3 \pm 1) \cdot 10^{-2} \text{ h}^{-1}$ and the Avogadro constant N_A is $6.02 \cdot 10^{23} \text{ mol}^{-1}$.

For 1 MeV radiation energy the relevant H_2O_2 concentration under realistic repository conditions is about only 10^{-6} mol/l .

Corrosion results for H₂O₂ at rest potentials

The results obtained in the various brines are compiled in Table II. The measured corrosion rates of Ti99.8Pd in saturated NaCl solution, Solution 3 (NaCl-rich brine) and Q-brine (MgCl₂-rich) at 25°C do not show any significant differences within the error limit. In all three systems a linear relationship exists between the corrosion rates and the H₂O₂ concentration. In a solution with an average H₂O₂ concentration of $2.9 \cdot 10^{-2}$ mol/l the corrosion rates are in the range from 22 to 28 µm/a. This specific H₂O₂ concentration is definitely higher than that expected under practical conditions and therefore it is only relevant with respect to basic research. At a H₂O₂ concentration of practical importance ($2.9 \cdot 10^{-5}$ mol/l) the corrosion rates are only 0.5 ± 0.3 µm/a. These values are only a little bit higher (by a factor of 1.5 - 2.0) than those obtained in H₂O₂ free solutions. At even smaller H₂O₂ concentrations ($\leq 10^{-5}$ mol/l) no influence of peroxide on Ti99.8Pd corrosion can be detected at all.

From earlier investigations [7] it can be seen that in solutions being free of H₂O₂, the corrosion is not influenced by temperatures up to 80°C. The corrosion rates are 0.4 ± 0.2 µm/a. Also in solutions containing peroxide, any increase of the corrosion cannot be obtained at 55°C. Corresponding measurements at 80°C are in progress.

All rest potentials are in the passive range. Attention should be paid to the fact that although the corrosion rates increase with increasing H₂O₂ concentration, the function rest potential vs. H₂O₂ concentration passes a minimum, which is due to different H₂O₂ influences on the anodic and cathodic partial current densities. The anodic current density is increased by TiO₂²⁺ formation shifting the rest potential to the negative range. The O₂ formation by H₂O₂ decomposition on the other hand increases the cathodic current density shifting the rest potential to more positive values, as can be seen from Figure 7.

Another main point of research is the investigation of Ti99.8-Pd TIG-welds. In order to answer the question whether the corrosive attack is higher on welds than on the parent material, measurements were carried out at rest potential at 25°C. The average H₂O₂ content of the solutions was $7 \cdot 10^{-3}$ mol/l. This high concentration is not relevant to practical conditions, but it is of high importance to know, whether there

are differences between metal and weld corrosion at all. Figure 8 shows that the corrosion rates of Ti99.8Pd welds are $5 \pm 1 \mu\text{m/a}$ in all three salt solutions, and therefore very close to the value of the unwelded material in saturated NaCl solution. These first measurements indicate that there are no differences in the corrosion behaviour of unwelded metal and Ti99.8Pd-welds at 25°C . The measurements will be continued at lower H_2O_2 concentrations.

Corrosion results for H_2O_2 at applied potentials

Investigations into corrosion of Ti99.8-Pd were carried out not only at rest potentials but also at various applied potentials from -1000 mV to $+1000 \text{ mV}$. From earlier measurements in saturated NaCl solution at 25°C and an average H_2O_2 concentration at $5 \cdot 10^{-2} \text{ mol/l}$, an active range was obtained between -400 mV and -1000 mV with maximum corrosion rates of $1500 \mu\text{m/a}$. The same experiments were carried out at 55°C and 80°C . The results are compiled in Table III. In the active range the corrosion increases further. The maximum corrosion rates are $2500 \mu\text{m/a}$ at 80°C . These values are not important from the practical but only from basic research point of view.

In the NaCl solution at 25°C containing an average H_2O_2 content of only $5 \cdot 10^{-3} \text{ mol/l}$, the relevant corrosion rates are definitely smaller ($30 - 40 \mu\text{m/a}$). This means the corrosion is reduced by a factor of 50. At a concentration $\leq 10^{-5} \text{ mol/l}$ no influence of H_2O_2 on corrosion of Ti99.8Pd can be detected, neither in the passive range nor in the active range.

Referring to these results, the question must be answered, whether the Ti99.8Pd shows the same behaviour in the salt solutions of practical importance (Solution 3, Q-brine) like in the model system saturated NaCl solution and which influences result from solution components Mg^{2+} or SO_4^{2-} .

Potentiostatic measurements in the range from -1000 mV to $+1000 \text{ mV}$ were carried out in Solution 3 and Q-Brine at 25°C . A high average H_2O_2 concentration ($5 \cdot 10^{-2} \text{ mol/l}$) was chosen to see differences between solutions with and without H_2O_2 . The

results are listed up in Table III. Neither in Solution 3 nor in Q-brine a marked active range can be obtained. In Solution 3 the maximum corrosion rates are $6 \pm 1 \mu\text{m/a}$, being only by a factor 2-3 higher than in peroxide free solution. In Q-brine containing H_2O_2 the corrosion rates equal those without any H_2O_2 ($2 \pm 1 \mu\text{m/a}$).

In order to find out the reason for this high resistance of Ti99.8Pd towards corrosion, the specific conductivity of the relevant oxide layers was determined. As was shown earlier, the corrosion corresponds to the specific conductivity of the protecting passive layers.

Figure 9 shows the obtained specific conductivities of the Ti99.8Pd passive layers at 25°C in saturated NaCl solution, Solution 3, Q-brine and in addition in Na_2SO_4 solution, MgCl_2 solution and NaCl solution containing Mg^{2+} or SO_4^{2-} ions. From Figure 9 it can be seen very clearly that in all solutions containing Mg^{2+} ions the specific conductivities of the protecting oxide layers are definitely lower than in saturated NaCl solution. The presence of SO_4^{2-} ions increases the specific conductivity. In Solution 3 the conductivity of the passive layer is influenced by Mg^{2+} and SO_4^{2-} , but not in Q-brine. The conductivity corresponds to that in MgCl_2 solution. The sulphate has not any influence. It can be supposed therefore that different oxide layers will be formed in presence of Mg^{2+} . Ilmenite or spinell structures can be assumed, which might hinder the corrosive attack. Detailed investigation should be performed in this area.

Influence of fluoride on the corrosion of Ti99.8-Pd

For a better interpretation of the results with H_2O_2 (cf. Figure 1) the corrosion was measured under the influence of F^- at rest potential and 25°C . If the corrosion is increased by a non decomposing reagent like NaF, forming TiF_6^{2-} -ions, the relevant corrosion rates should increase and the rest potential should decrease. F^- should have no influence on the cathodic current density.

From the corrosion rates listed up in Table II, it can be seen, that the corrosion rates increase with increasing F^- -concentration, being in accordance with the behaviour of

H₂O₂ containing brines. But in contrast to H₂O₂, the rest potentials decrease with increasing F⁻-content of the solution. This behaviour is in accordance with the theory. A minimum of the rest potential curve cannot be obtained therefore.

Influence of ClO⁻ on the corrosion of Ti99.8-Pd

Another product of radiolysis in salt solution is the hypochlorite ClO⁻, which can influence the corrosion behaviour of the Ti99.8Pd. In order to see whether there is a difference between the corrosion of Ti99.8-Pd (TiGrade7) in solutions with and without ClO⁻, a very high ClO⁻ concentration of 0.08 mol/l was used. This high ClO⁻ concentration is not relevant to practical conditions, of course. It is only relevant to basic research.

Potentiostatic measurements were carried out in the potential range from -1000 mV to +1000 mV at 25°C in saturated NaCl solution containing 0.08 mol/l ClO⁻. Neither at anodic polarization nor at cathodic polarization the corrosion rates are higher than in the solutions being free of ClO⁻ (see Table 3). In the whole potential range, corrosion rates of 3±1µm/a are measured. From these results it can be concluded that ClO⁻ has no influence on the corrosion behaviour of Ti99.8Pd.

C.1.3 Stress corrosion cracking studies in salt and granite environments (Work Packages 1 and 2) (ENRESA/INASMET)

The resistance of three candidate container materials to stress corrosion cracking (SCC) is investigated in NaCl brine (26.9 wt.% NaCl) and in bentonite buffered granitic groundwater at 170°C and 90°C, respectively, by means of the slow strain rate technique (SSRT).

The materials to be studied have the following compositions (wt.%):

Carbon steel TStE355: 0.16 C; 0.41 Si; 1.5 Mn; 0.017 P; 0.002 S; bal. Fe

Stainless steel AISI 316L: 17.4 Cr; 11.5 Ni; 2.2 Mo; 0.021 C; 0.31 Si; 1.3 Mn; bal. Fe

Ti99.8-Pd (TiGr-7): 0.15 Pd; 0.040 C; 0.003 H; 0.04 Fe; 0.12 O; bal. Ti

Besides the parent metals, welded joints simulating potential container closure techniques are also considered. These are:

- EBW (Electron Beam Welding) for the three candidate container materials.
- FCAW (Flux Cored Arc Welding) for the carbon steel.
- PAW (Plasma Arc Welding) for the titanium alloy.
- GTAW (Gas Tungsten Arc Welding) for the stainless steel.

Following test conditions are applied:

SALT BRINE 170°C:

- TStE355 steel: Strain rates ranging from 10^{-4} to 10^{-7} s $^{-1}$.
- Ti99.8-Pd alloy (TiGr-7): Strain rates of 10^{-6} and 10^{-7} s $^{-1}$.

GRANITIC GROUND WATER 90°C:

- TStE355 steel: Strain rates ranging from 10^{-4} to 10^{-7} s $^{-1}$.
- AISI 316L steel: Strain rates ranging from 10^{-4} to 10^{-7} s $^{-1}$.

In addition, comparative tests are performed in argon as an inert reference medium.

During the reporting time, slow strain rate tests have been performed on the TStE355 carbon steel in synthetic bentonite granitic water and argon at 90°C, and strain rates ranging from 10^{-4} to 10^{-7} s $^{-1}$. The steel was investigated both in the parent condition and in the welded conditions EBW and FCAW. The chemical composition and pH of the synthetic bentonite granitic water are given in Table IV.

Experimental

For the slow strain rate tests on the steel, round specimens of 6mm diameter and 30mm gauge length were used. The experiment equipment used is described in a previous work [8]. Shortly, the specimens were located in Hastelloy C-276 autoclaves with one end being attached to fixed frame and the other to the pull rod. Then, the autoclaves were filled either with brine or argon, closed, pressured and heated. Once the testing temperature (90°C) and pressure (13 MPa) were reached, the specimens pulled until fracture at the selected actuator displacement speed.

Load, position, time and temperature data were continuously logged by the

microprocessor that controls the testing machine. After each test, the elongation (E), reduction of area (R.A.), energy, yield strength (Y.S.), maximum load, and true stress at fracture were determined. To evaluate the resistance of the steel to SCC, metallographic and scanning electron microscopic (SEM) examinations of specimens were performed, in addition to the tensile experiments.

Results

The results obtained for welded and unwelded steel specimens in argon and granitic water at 90°C and strain rates of 10^{-4} to 10^{-7}s^{-1} are given in Figure 10. The comparison of the results in these two media shows that the steel suffers a loss of ductility in granite environment. This is mainly noticed in the decrease of the reduction of area and true stress at fracture in granitic water. The drop of these parameters is not significant at the highest strain rate of 10^{-4}s^{-1} but it is important at the lower strain rates used in these experiments. The values of the yield strength and the maximum load in granitic water are very close to those in argon. Considering the welded specimens, the fracture was located in the base material. Figure 11 shows macrographs of TstE355 steel specimens tested in argon and granitic water at 90°C and a strain rate of 10^{-7}s^{-1} .

In the metallographic examinations of the unwelded steel specimens, no clear signs of sensitivity to SCC in the granitic water was found. On the lateral surface of the specimens (Figure 12) areas of non-uniform general corrosion due to the local and repetitive breaking of the oxide layer were observed. X-Ray Diffraction (XRD) analysis of the oxide layer shows that it is magnetite (Fe_3O_4). Metallographic examinations of the welded steel specimens are currently underway.

SEM examinations of the fracture surface show a brittle appearance for specimens tested in the granitic medium (Figure 13), and a fully ductile surface for specimens examined in argon. The loss of ductility shown by the carbon steel in the granite environment is attributed to the embrittling effect of the corrosion hydrogen produced on the specimens surface during the test. This is interpreted as a Hydrogen Assisted Stress Cracking (HASC) phenomenon.

C.2 Corrosion studies in clay/bentonite environments (Work package 3) (SCK.CEN)

In addition to previous in-situ corrosion experiments [9], electrochemical corrosion studies are performed on candidate container materials aimed at investigating the influence of important environmental parameters on localized corrosion. Such parameters are: the temperature (16°C - 90°C) and the content of O₂, Cl⁻, SO₄²⁻ and S₂O₃²⁻ of the corrosion medium. The corrosion medium is oxidizing synthetic interstitial clay water having the following composition in wt.%;

1.01 Mg²⁺; 10.2 SO₄²⁻; < 15 K⁺; 49.7 Cl⁻; 413 Na⁺; 1.62 F⁻; 832 HCO₃⁻/CO₃²⁻;
5.86 Ca²⁺.

Materials and experimental

The materials under investigation are compiled in Table V. The emphasis is laid on the study of carbon steel and stainless steels, as these materials are the most important in the current disposal concept. Nevertheless, some higher alloyed stainless steels, the nickel base alloy Hastelloy C4, and the titanium alloy Ti99.8-Pd (Ti/0.2Pd, Ti-grade 7) are investigated too, albeit to a less extent.

The electrochemical experiments are performed in a corrosion cell (EG&G model K0047), containing a working electrode, a Ag/AgCl reference electrode with Luggin capillary, and two graphite counter electrodes. Various preparation techniques for the working electrode were evaluated on their ability to eliminate crevice corrosion. Potential sequences (potentiodynamic or potentiostatic) are applied to the electrochemical system with a EG&G model 273A potentiostat/galvanostat.

The corrosion behaviour of the container materials was investigated by recording polarization curves of the studied alloys in clay water. From the polarization curves, the characteristic pitting potentials E_{np} and E_{pp} were determined. E_{np} , the critical potential for pitting, is the potential above which new pits are initiated. E_{pp} , the protection potential, is the potential above which existing pits grow but no new pits are nucleated. To assess the influence of environmental parameters on the pitting

corrosion, the chloride, sulphate and thiosulphate content of the clay water were varied independently. To investigate the influence of temperature, tests were performed at 16°C and 90°C.

Since crevice corrosion can complicate the interpretation of polarisation curves, a crevice-free working electrode was developed. As reported earlier [4], several preparation methods were tried before, but electrochemical tests showed that none of them was completely successful in avoiding crevices between the metallic sample and the working electrode holder.

In 1997, two new types of working electrodes were examined: the 'rod' type electrode and the 'Epoxipatch' type electrode. The 'rod' type working electrode is easily fabricated and allows to work crevice-free but has some disadvantages. To make this electrode, rectangular rods are cut from a plate of the investigated alloy. The rods are then polished and connected to the potentiostat. Since there is no electrode holder, no crevices can exist between the working electrode and the holder. However, this method has two disadvantages. Firstly, rectangular rods are difficult to polish. Secondly, the immersed surface area of the electrode depends on the level of the electrolyte. As the water level can change during stirring of the electrolyte, stirring cannot be used with the 'rod' type electrode. Because of these difficulties, the use of this electrode was abandoned.

The 'Epoxipatch' electrode is prepared by subsequent embedding circular specimens in two different epoxy resins. The first resin is used for an optimal wetting of the metallic sample. The second resin, which is a cold mounting epoxy resin, allows to obtain working electrodes that can be automatically polished. The disadvantages mentioned for the 'rod' type working electrode do not occur for the 'Epoxipatch' electrode. The electrode's surface area is determined by the diameter of the metallic sample and stirring of the electrolyte is possible. Therefore, this type of working electrode was used for all the electrochemical experiments.

Influence of temperature

The pitting corrosion behaviour of the investigated alloys depends on temperature. The higher the temperature, the more likely pitting corrosion will occur. At 16°C, the carbon steel was the only material which exhibited corrosion. None of the other alloys showed any form of corrosion, neither localized nor general. At 90°C the corrosion behaviour depends on the alloy composition and the anion content of the electrolyte. In synthetic oxidized clay water with a chloride content of 100 ppm and a sulphate content of 216 ppm, which is the reference electrolyte, pitting occurs for carbon steel, but not for the other candidate container materials.

Influence of chloride concentration

The resistance of the investigated alloys to pitting corrosion depends on the chloride concentration of the clay water. Table VI shows the critical pitting potentials E_{np} and E_{pp} as function of chloride concentration, expressed as their relative position (in mV), with respect to the corrosion potential or open circuit potential. These values are a measure for the pitting resistance of the alloys. From these results it can be concluded that a higher chloride content decreases the pitting resistance of all alloys. The only alloy that exhibits no pitting at all is Hastelloy C4, which makes it the most suitable as container material. Also, from the results in Table VI, a classification according to decreasing pitting resistance can be made:

Hastelloy C4 > Cronifer 1925 hMo > UHB 904L > AISI 316L hMo > AISI 316L > TStE 355

When considering this classification one should bear in mind that Ti/0.2Pd has not yet been investigated.

Influence of sulphate concentration

The increase of the sulphate concentration in the clay water, increases the pitting resistance of the investigated candidate container materials. This can clearly be seen in Table V, which summarizes the results of pitting tests as function of the chloride and sulphate concentration. This conclusion is valid for all investigated alloys. A high

sulphate concentration is typical of oxidized clay water. Indeed, during the oxidation of clay water, the sulphate content rises and the pH drops.

Influence of thiosulphate concentration

The influence of thiosulphate on the pitting corrosion behaviour has up to now only been studied for AISI 316L, AISI 316L hMo, and UHB 904L. Table VII lists the results of the electrochemical tests in synthetic oxidized clay water with 100 ppm chloride and 216 ppm sulphate, and with varying thiosulphate content.

For AISI 316L, the resistance to pitting corrosion decreases with increasing thiosulphate content of the clay water. For AISI 316L hMo and UHB 904L, higher thiosulphate content does not have this effect. The pitting resistance of AISI 316L hMo is not influenced by a thiosulphate content variation between 2 and 50 ppm. The pitting resistance of UHB 904L even increases at a thiosulphate content of 50 ppm. Due to the limited number of experiments performed, it is still too early to explain the behaviour of the studied alloy in the presence of thiosulphate.

D. CONCLUSIONS

Initial pH values of 1–5 of the NaCl-rich test brine ($T = 170^{\circ}\text{C}$) do not influence significantly the corrosion rate of the TStE355 carbon steel ($42\text{--}50\ \mu\text{m/a}$). At higher pH (6–10) the corrosion rates decrease by a factor of 1.5 – 1.8. Chemical species in the NaCl-rich brine environment such as $\text{B}(\text{OH})_4^-$ and Fe^{3+} accelerate the corrosion rate of the steel at 90°C and 170°C . The radiolytic products H_2O_2 and ClO^- increase the corrosion rate only at 90°C .

The corrosion rate of Ti99.8-Pd in salt brines ($T = 25^{\circ}\text{C} - 80^{\circ}\text{C}$) increases with increasing content of H_2O_2 , ClO^- and F^- . However, realistic concentrations of these species in disposal brines ($10^{-5} - 10^{-4}\ \text{mol/l}$) do not increase the corrosion rate of this alloy over the values in the „pure brines“.

In granite environment at 90°C and strain rates of $10^{-4} - 10^{-7}\ \text{s}^{-1}$, the TStE355 steel is not susceptible to stress corrosion cracking. However, the steel suffers under these

conditions a loss of ductility which is attributed to the embrittling effect of the corrosion hydrogen.

In clay water ($T = 16^{\circ}\text{C}$, 90°C), the increase of temperature and chloride content decreases the resistance of the test materials (carbon steel, stainless steels, Hastelloy C4) to pitting corrosion. On the contrary, the higher the SO_4^{2-} content in the clay water the higher the resistance of the materials to pitting. The influence of $\text{S}_2\text{O}_3^{2-}$ to pitting corrosion depends on the alloy. Among the materials investigated Hastelloy C4 has the highest resistance to pitting corrosion.

E. PLANNED WORK FOR THE NEXT REPORTING PERIOD

Corrosion studies in salt environments (Work Package 1)

- Continuation of the long-term immersion experiments into the effect of chemical species on the corrosion of TStE355 carbon steel in brines. Investigations at high temperature (170°C) in the MgCl_2 -rich „Q-brine“ containing selected salt impurities and radiolytic products.
- Further electrochemical corrosion studies on Ti99.8-Pd at higher temperatures (55°C and 80°C) and various potentials in NaCl -rich and MgCl_2 -rich brines containing H_2O_2 concentrations of $10^{-5} - 10^{-2}$ mol/l. Characterization of the protecting oxide surface layer by electrochemical and impedance measurements.

Stress corrosion cracking studies in granite environments (Work Package 2)

Slow strain rate tests on the AISI 316L stainless steel in bentonite buffered granitic ground water at 90°C and strain rates of $10^{-4} - 10^{-7}\text{s}^{-1}$.

Corrosion studies in clay/bentonite environments (Work Package 3)

Conclusion of the electrochemical studies in synthetic oxidizing clay water into the influence of various parameters (Cl^- , SO_4^{2-} , $\text{S}_2\text{O}_3^{2-}$) on the pitting corrosion of container materials. Start of corresponding studies in bentonite buffered water.

F. REFERENCES

- [1] MARSH, G.P., PINARD-LEGRY, G., SMAILOS, E. et al. „HLW Container Corrosion and Design,“ Proc. of the Second European Community Conference on Radioactive Waste Management and Disposal, Luxembourg, April 22-26, 1985, p. 314, SIMON R.A., Ed., Cambridge University Press (1986).
- [2] SMAILOS, E., SCHWARZKOPF, W., KÖSTER, R. and GRÜNTHALER, K.H., „Advanced Corrosion Studies on Selected Packaging Materials for Disposal of HLW Canisters in Rock Salt,“ Proc. of the Symposium on Waste Management 1988 at Tucson, Arizona, USA, February 28 – March 3, 1988, Vol.2, p. 985.
- [3] SMAILOS, E., AZKARATE, I., GAGO, J.A., Van ISEGHEM, P., KURSTEN, B., McMENAMIN, T., „Corrosion Studies on Metallic HLW Container Materials,“ Presented at the Fourth Conference of the European Commission on the Management and Disposal of Radioactive Waste, Luxembourg, 25-29 March 1996.
- [4] SMAILOS, E., GAGO, J.A., Kursten, B., Marx, G., AZKARATE, I., „Corrosion Evaluation of Metallic Materials for Long-Lived HLW/Spent Fuel Disposal Containers,“ FZKA Report No. 5889 (1997).
- [5] SMAILOS, E., „Corrosion of High-Level Waste Packaging Materials in Disposal Relevant Brines,“ Nuclear Technology, Vol. 104, p. 343, 1993.
- [6] HENGLEIN, A., SCHNABEL, W., WENDENBURG, J., „Einführung in die Strahlenchemie“, Verlag Chemie, Weinheim (1996).
- [7] MARX, G., NEHM, C., „Radiochemische Korrosionsuntersuchungen an Titan und Titanlegierungen als Containerwerkstoffe in praxisrelevanten Salzlaugen,“ Final Report of the FU Berlin to the BMFT Project FZK02E82613, 1995.
- [8] SMAILOS, E., GAGO, J.A., AZKARATE, I., FIEHN, B., „Corrosion Studies on Selected Packaging Materials for Disposal of Heat-Generated Radioactive Wastes in Rock-Salt Formations,“ FZKA Report No. 5587, 1995.
- [9] KURSTEN, B., CORNELIS, B., LABAT, S., Van ISEGHEM, P., „Completion of the Corrosion Programme in Boom Clay-In-situ Experiments – Nuclear Science and Technology, EUR 17105 EN, 1997.

Table I: Chemical species examined in the corrosion studies on TStE 355 steel in salt brines

Species	Added to the brine as	Concentration mol/l
$B(OH)_4^-$	H_3BO_3	$1.4 \cdot 10^{-1}$
Fe^{3+}	$FeCl_3 \cdot 6H_2O$	$3.5 \cdot 10^{-2}$
H_2O_2	15% H_2O_2 -solution	10^{-3} ; 10^{-2}
ClO^-	15% $NaClO$ -solution	10^{-3}

Table II: Corrosion rates of Ti99.8-Pd in brines containing H_2O_2 and F^- at rest potentials

Solution	Initial H_2O_2 concentration (mol/l)	Average H_2O_2 concentration (mol/l)	F^- concentration (mol/l)	Corrosion rates (25°C) ($\mu m/a$)	Corrosion rates (55°C) ($\mu m/a$)
sat. NaCl	0	0	---	0.3 ± 0.2	0.3 ± 0.2
	$7.0 \cdot 10^{-5}$	$2.9 \cdot 10^{-5}$	---	0.6 ± 0.3	0.6 ± 0.2
	$7.0 \cdot 10^{-4}$	$2.9 \cdot 10^{-4}$	---	0.5 ± 0.3	0.7 ± 0.3
	$3.5 \cdot 10^{-3}$	$1.5 \cdot 10^{-3}$	---	1.0 ± 0.3	2.1 ± 0.7
	$7.0 \cdot 10^{-3}$	$2.9 \cdot 10^{-3}$	---	1.8 ± 0.5	1.5 ± 0.7
	$3.5 \cdot 10^{-2}$	$1.5 \cdot 10^{-2}$	---	10 ± 2	5 ± 1
	$7.0 \cdot 10^{-2}$	$2.9 \cdot 10^{-2}$	---	22 ± 2	21 ± 2
Solution 3	0	0	---	0.4 ± 0.2	0.3 ± 0.2
	$7.0 \cdot 10^{-5}$	$2.9 \cdot 10^{-5}$	---	0.9 ± 0.2	0.2 ± 0.2
	$7.0 \cdot 10^{-4}$	$2.9 \cdot 10^{-4}$	---	0.5 ± 0.1	0.5 ± 0.1
	$3.5 \cdot 10^{-3}$	$1.5 \cdot 10^{-3}$	---	0.9 ± 0.1	0.5 ± 0.2
	$7.0 \cdot 10^{-3}$	$2.9 \cdot 10^{-3}$	---	4 ± 2	---
	$3.5 \cdot 10^{-2}$	$1.5 \cdot 10^{-2}$	---	4.0 ± 0.5	---
	$7.0 \cdot 10^{-2}$	$2.9 \cdot 10^{-2}$	---	17 ± 4	14 ± 10
Q-brine	0	0	---	0.4 ± 0.2	0.4 ± 0.3
	$7.0 \cdot 10^{-5}$	$2.9 \cdot 10^{-5}$	---	0.6 ± 0.2	---
	$7.0 \cdot 10^{-4}$	$2.9 \cdot 10^{-4}$	---	0.3 ± 0.1	---
	$3.5 \cdot 10^{-3}$	$1.5 \cdot 10^{-3}$	---	0.6 ± 0.1	---
	$7.0 \cdot 10^{-3}$	$2.9 \cdot 10^{-3}$	---	0.7 ± 0.1	---
	$3.5 \cdot 10^{-2}$	$1.5 \cdot 10^{-2}$	---	3.7 ± 0.8	---
	$7.0 \cdot 10^{-2}$	$2.9 \cdot 10^{-2}$	---	21 ± 4	---
sat. NaCl	---	---	$3.3 \cdot 10^{-3}$	0.1 ± 0.1	---
	---	---	$6.7 \cdot 10^{-3}$	0.9 ± 0.3	---
	---	---	$3.3 \cdot 10^{-2}$	5.3 ± 0.5	---
	---	---	$6.7 \cdot 10^{-2}$	11.5 ± 0.5	---

Table III: Corrosion rates of Ti99.8-Pd in brines containing H₂O₂ and ClO⁻ at various applied potentials

Solution	sat. NaCl					Solution 3	Q-brine
average H ₂ O ₂ conc. (mol/l)	---	5.0·10 ⁻³	5.0·10 ⁻²			---	5.0·10 ⁻²
ClO ⁻ conc. (mol/l)	---	---	---			8·10 ⁻²	---
Temp. (°C)	25	25	25	55	80	25	25
Potential (mV)	corr. rate (μm/a)	corr. rate (μm/a)	corr. rate (μm/a)	corr. rate (μm/a)	corr. rate (μm/a)	corr. rate (μm/a)	corr. rate (μm/a)
-1000	1±1	2±1	1±1	1±2	1±2	2±1	2±1
-500	3±2	1±1	104±9	331±103	143±50	1±2	1±1
-400		4±2	513±87	539±81	2159±150	3±1	2±1
-350		32±13	611±59	2482±344	4151±232		2±1
-300		10±6	1441±15	2824±311	2243±167	2±1	1±1
-250	5±1	10±5	792±34	1979±177	1323±145		2±1
-200		2±1	450±9	1270±170	1282±150	1±1	2±2
-150		1±1	384±21	995±14	948±124		2±1
-100		2±1	38±16	271±7	372±99	1±1	1±1
0	1±2	1±1	10±8	3±2	6±5	1±2	2±1
500	1±2	1±1	4±2	8±2	29±10	1±1	2±1
1000		1±1	1±1	1±1	2±2		1±1

Table IV: Chemical composition (limits) of the synthetic bentonite-granitic water

Species	Concentration(mg/l)
Cl ⁻	6550±250
NO ₃ ⁻	110±10
SO ₄ ²⁻	1500±30
HCO ₃ ⁻	27±5
SiO ₂	8.3±0.5
Br ⁻	15±1
Ca ²⁺	135±10
K ⁺	20±1
Mg ²⁺	600±30
Na ⁺	3750±100
pH	7.3

Table V. Chemical composition of the container materials tested in clay environments

	Chemical composition (wt%)										
	Fe	Cr	Ni	Mn	Mo	Si	Ti	C	S	P	Others
<u>Carbon steel</u>											
TSSt 355	bal	0.03	0.03	1.12	0.00	0.34	0.003	0.180	0.002	0.010	Nb 0.017; N ₂ 0.005
<u>Stainless steels</u>											
AISI 316L	bal	16.9	11.0	1.54	2.08	0.54	-	0.017	0.001	0.032	
AISI 316LhMo	bal	17.6	12.5	1.16	2.84	0.61	-	0.015	0.001	0.030	
AISI 316Ti	bal	16.8	10.7	1.08	2.05	0.40	0.3	0.044	0.009	0.028	
<u>Higher alloyed stainless steel</u>											
UHB 904L											
Cronifer	bal	19.7	25.0	1.48	4.47	0.19	-	0.019	0.001	0.019	Cu1.5;N ₂ 0.08
1925hMo	45.4	20.6	24.8	0.92	6.40	0.30	-	0.005	0.002	0.018	Cu0.86;N ₂ 0.19
<u>Nickel alloy</u>											
Hastelloy C4	0.98	15.7	67.0	0.04	15.8	0.02	<0.01	0.003	0.003	0.004	Co:0.01
<u>Titanium alloy</u>											
Ti/0.2Pd	0.04	-	-	-	-	-	bal	0.010	-	-	Pd:0.16;O ₂ :0.1 N ₂ <0.01; H ₂ :0.001

Table VI: Influence of chloride and sulphate content on the critical pitting potentials for the investigated candidate container materials at 90°C in synthetic oxidized clay water (all potentials in mV versus E_{corr}).

[SO ₄ ²⁻] (ppm)	[Cl ⁻] (ppm)	TSSt 355	AISI 316L	AISI316LhMo	UHB 904L	Cronifer 1925 hMo	Hastelloy C4
216	100	uniform corrosion	no pitting	no pitting	no pitting	no pitting	no pitting
216	1000	uniform corrosion	E _{np} 626 E _{pp} 230	E _{np} 390 E _{pp} 120	E _{np} 750 E _{pp} 330	no pitting	no pitting
216	10000	uniform corrosion	E _{np} 418 E _{pp} 84	E _{np} 375 E _{pp} 100	E _{np} 440 E _{pp} 65	E _{np} 794 E _{pp} 42	no pitting
5400	100	uniform corrosion	not investigated	no pitting	no pitting	not investigated	not investigated
5400	1000	uniform corrosion	no pitting	no pitting	no pitting	not investigated	not investigated
5400	10000	uniform corrosion	E _{np} 730 E _{pp} 81	E _{np} 280 E _{pp} 65	E _{np} 490 E _{pp} 190	not investigated	not investigated

Table VII: Characteristic pitting potentials for UHB 904L in synthetic oxidized clay water containing 100 ppm Cl⁻ and 216 ppm SO₄²⁻ as a function of thiosulphate content of the clay water.

[S ₂ O ₃ ²⁻] (ppm)	AISI 316L		AISI 316L hMo		UHB 904L	
	E _{np}	E _{pp}	E _{np}	E _{pp}	E _{np}	E _{pp}
2	619	50	687	412	891	438
20	590	189	701	285	870	385
50	438	-40	711	731	1034	475

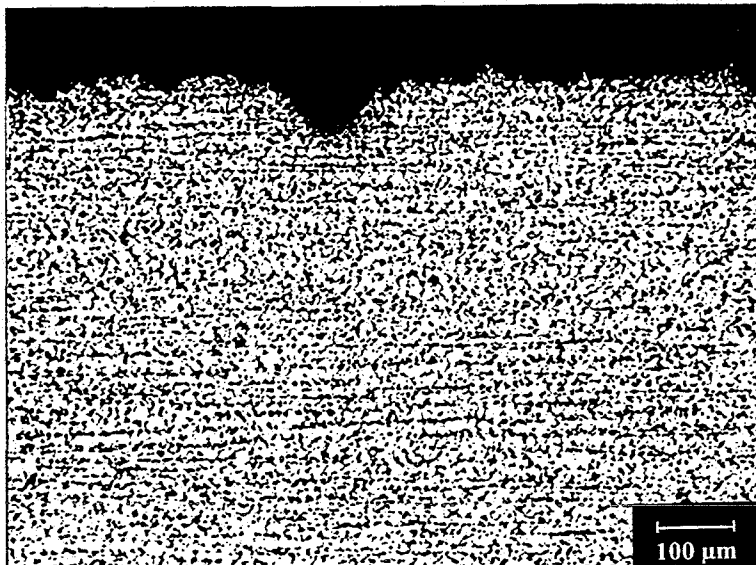


Figure 1. pH1

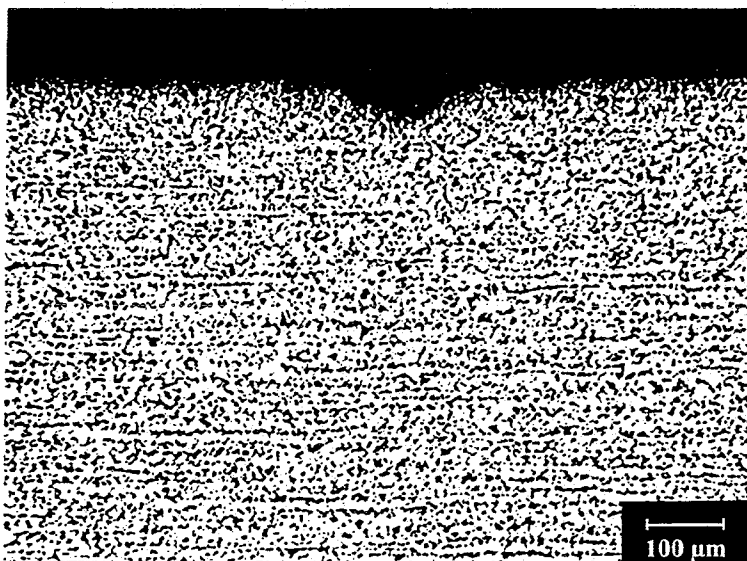


Figure 2. pH10

Figures 1-2: Optical micrographs of TStE 355 steel after 1 year exposure to NaCl-rich brine at 170°C and various pH values

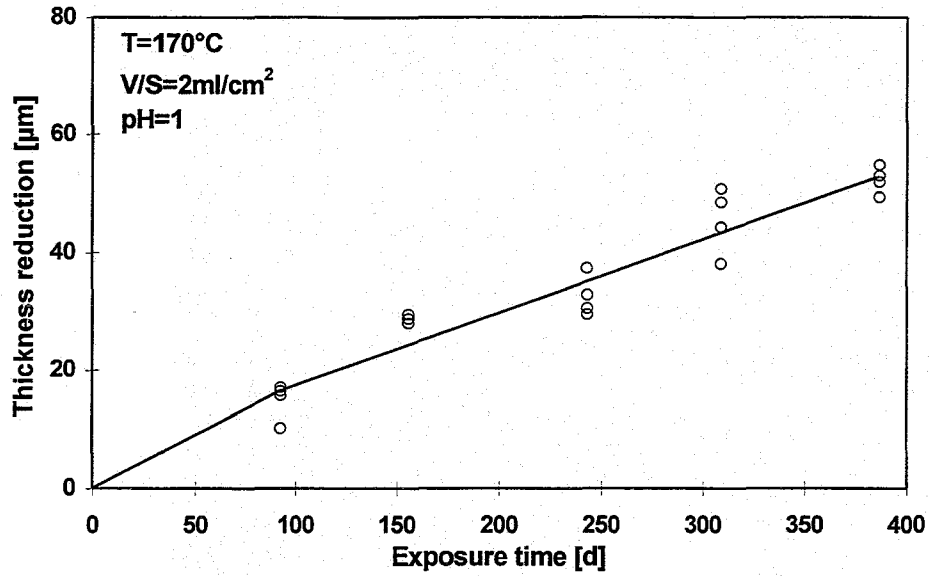


Figure 3: Time-dependence of the thickness reduction of TStE355 steel in NaCl-rich brine at 170°C and pH=1

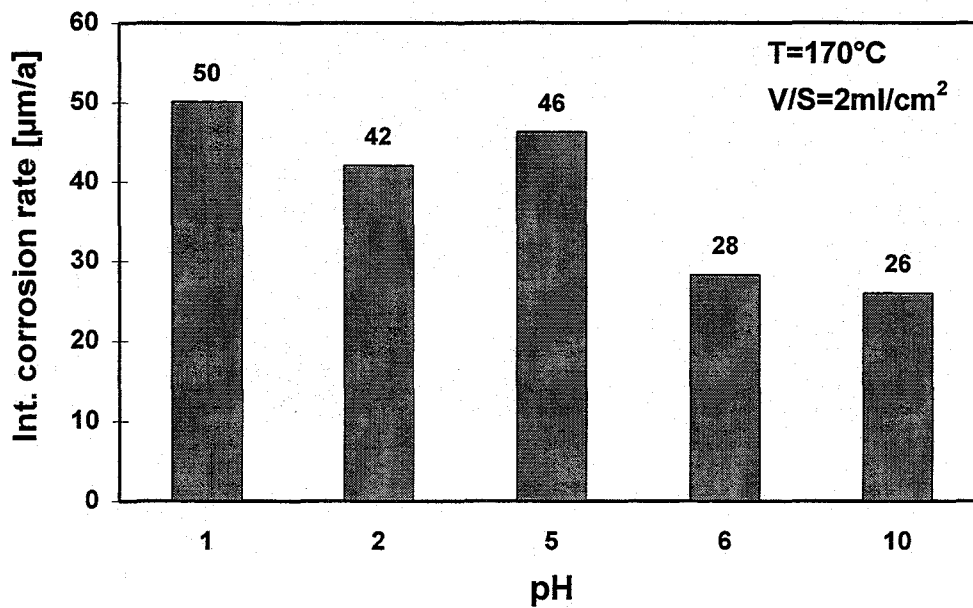


Figure 4: Corrosion rates of TStE 355 steel as a function of pH in NaCl-rich brine at 170°C

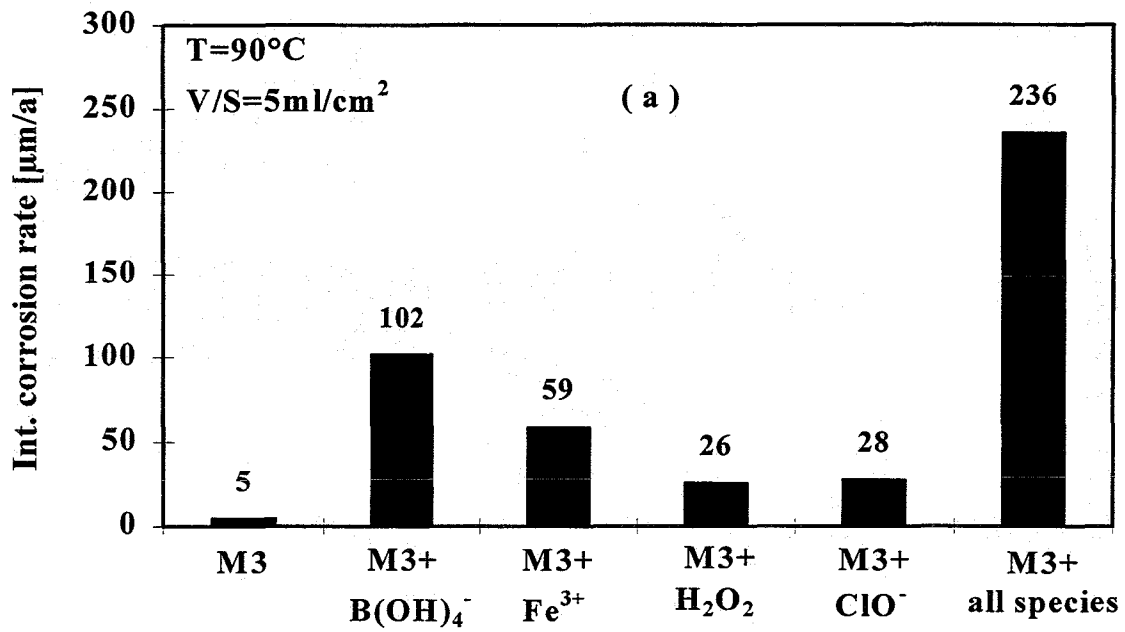


Figure 5

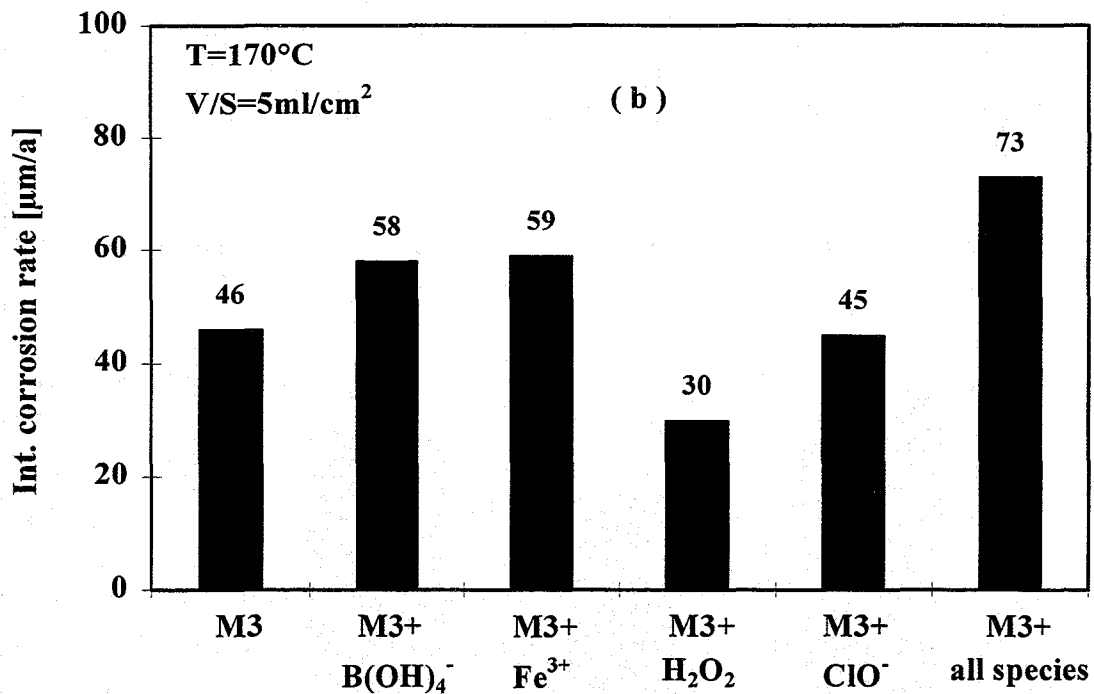


Figure 6

Figures 5-6: Corrosion rates of TStE355 steel at 90°C and 170°C in NaCl-rich brine (M3) with and without additions of chemical species

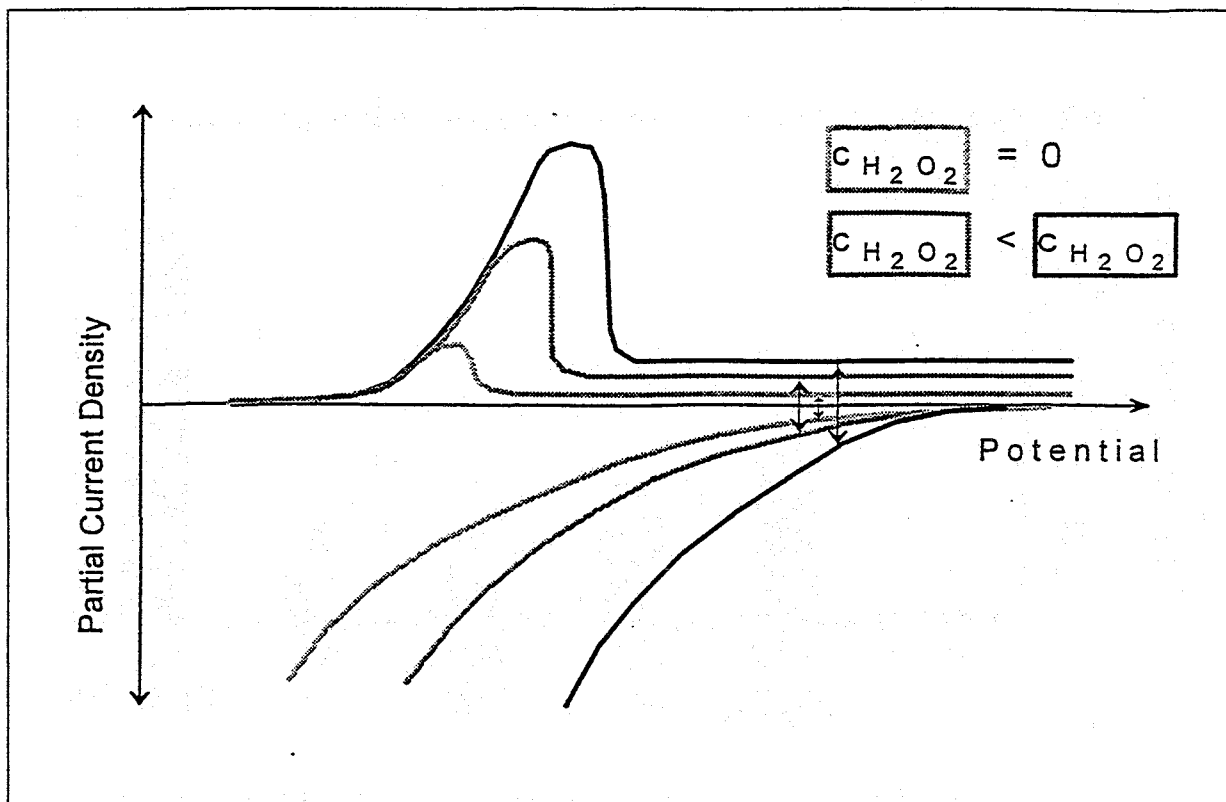


Figure 7: Shift of the rest potential of Ti99.8-Pd in presence of H_2O_2 in the brines (25°C)

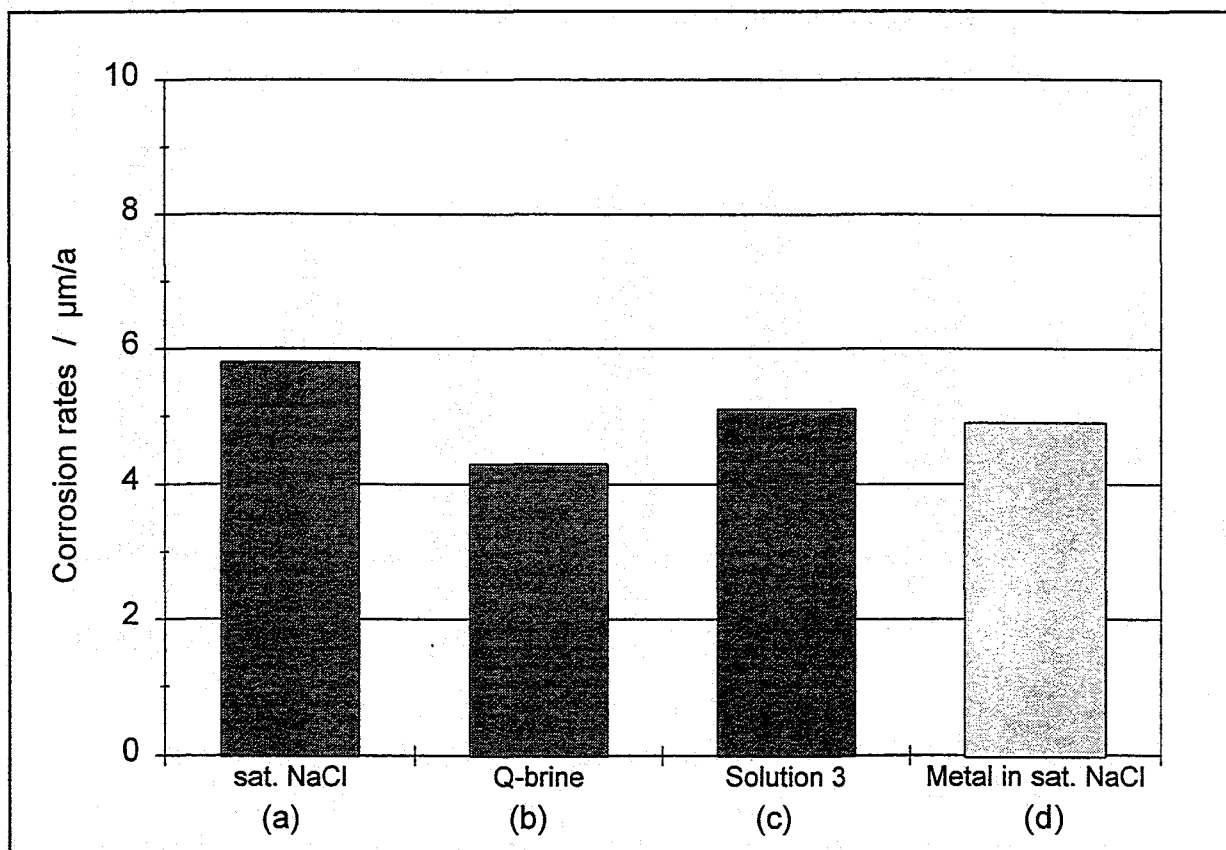


Figure 8: Corrosion rates of TIG-welded (a,b,c) and unwelded (d) Ti99.8-Pd in brines containing H_2O_2 (average concentration: 0.007 mol/l; T=25°C)

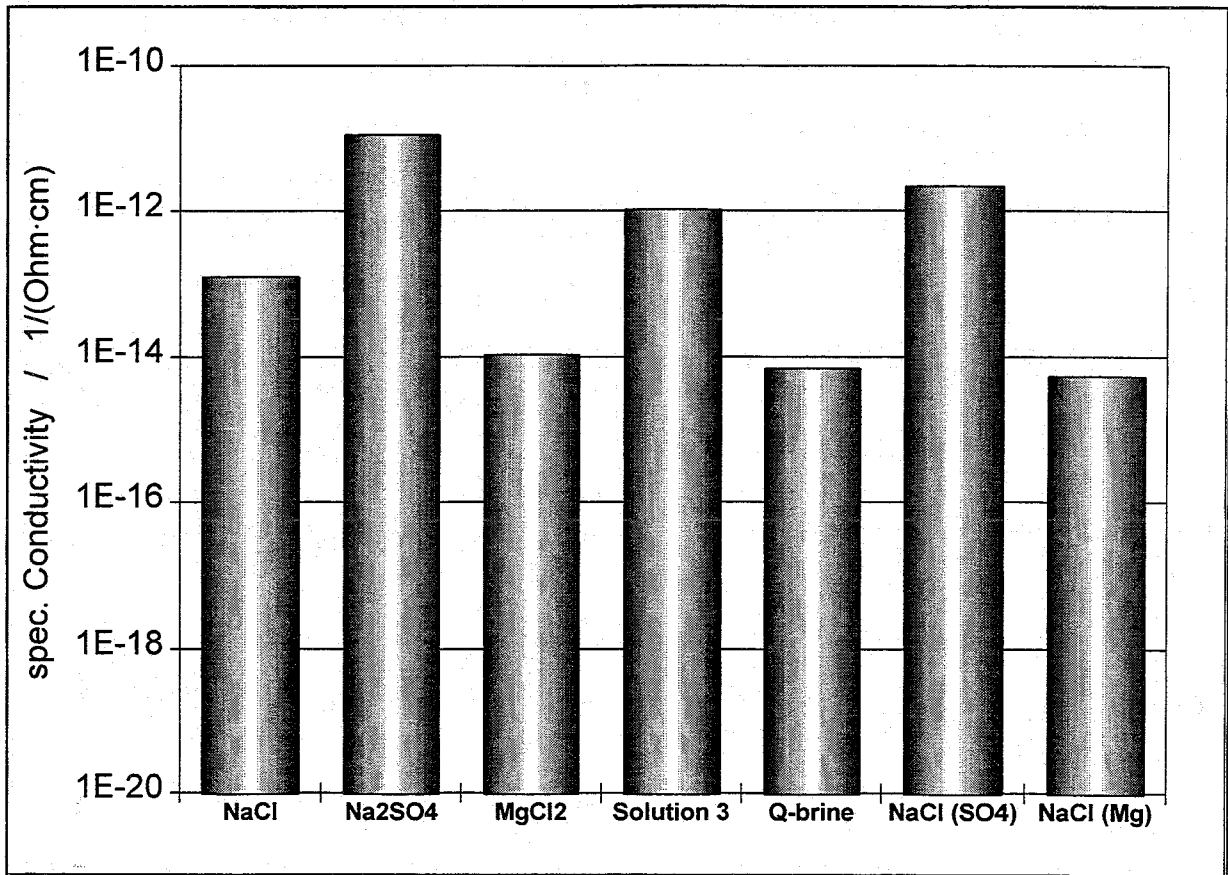
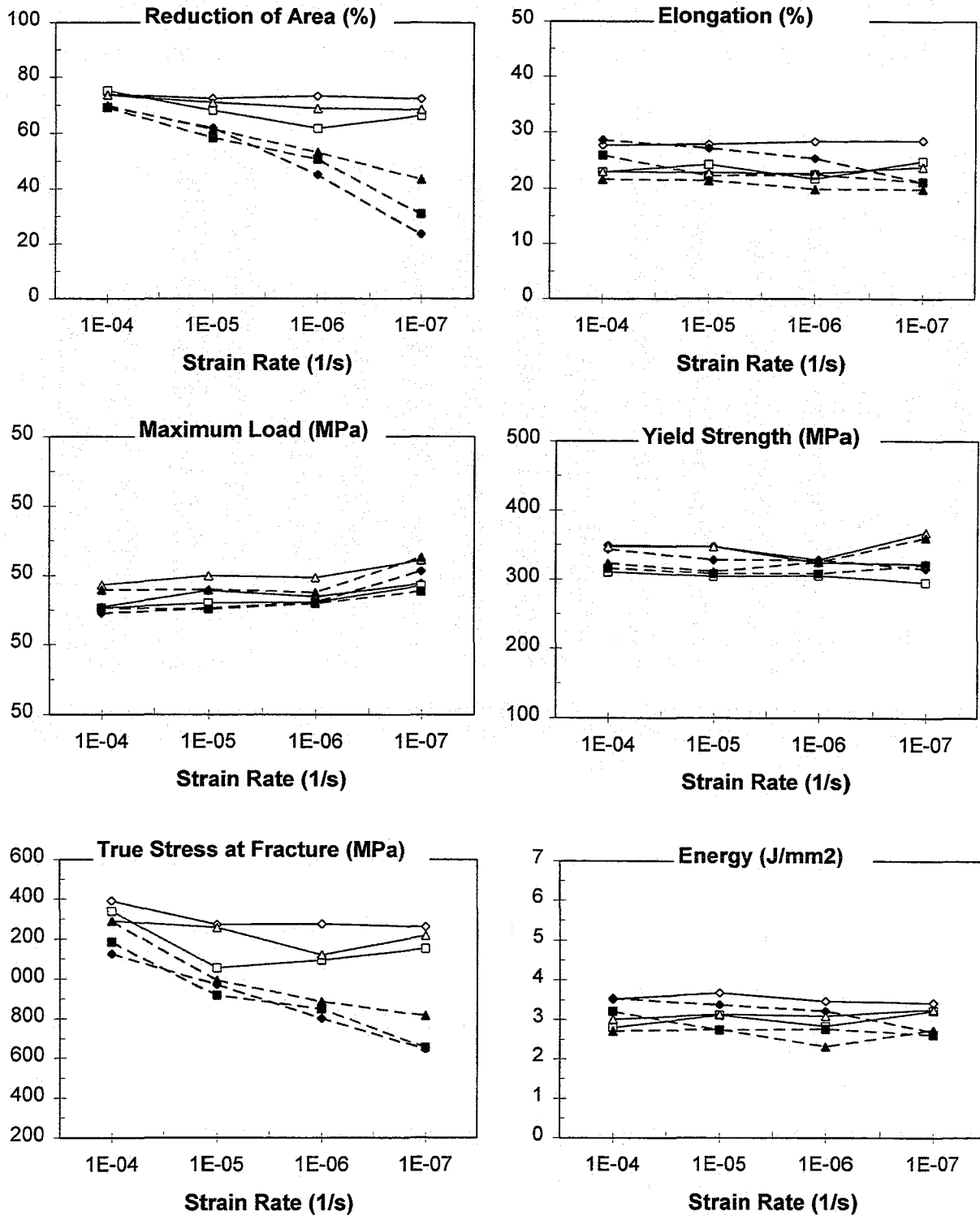


Figure 9: Specific conductivities of the oxide layers formed on Ti99.8-Pd in various salt brines ($U=2\text{V}$; 25°C)



—◇— 355 Argon —◆— 355 Granite —□— 355(EBW) Argon —■— 355(EBW) Granite —△— 355(FCAW) Argon —▲— 355(FCAW) Granite

Figure 10: Elongation, reduction of area, energy, yield strength, maximum load and true stress fracture values versus strain rate for the parent and welded TStE355 steel, tested at 90°C in argon and granitic water.

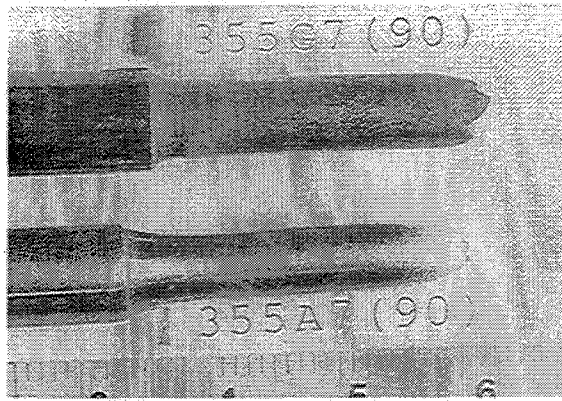


Figure 11: Macrographs of two TStE355 steel tensile specimens tested in argon and granitic water at 90°C and a strain rate of 10^{-7}s^{-1}

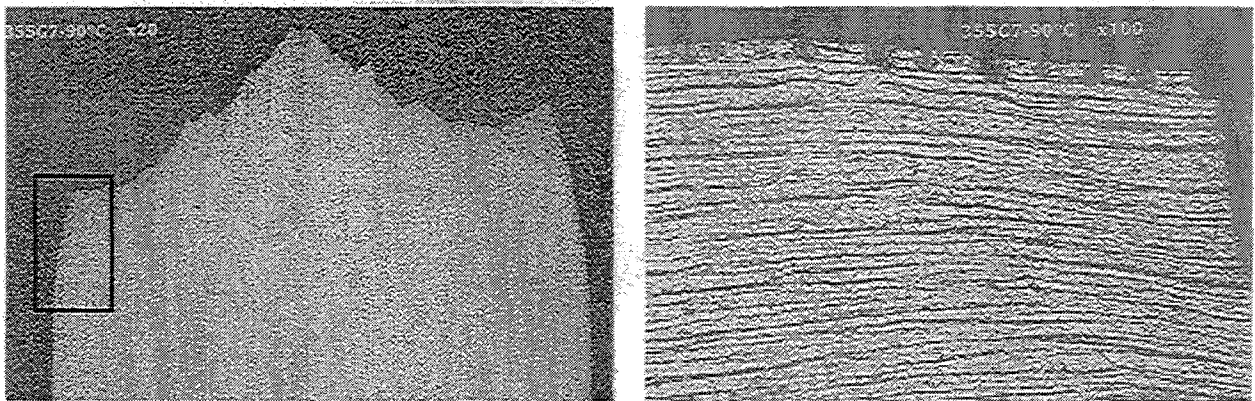


Figure 12: a) Optical micrograph of a tensile specimen of parent TSt E355 steel tested at a strain rate of 10^{-7}s^{-1} in granitic water at 90°C (x16); b) Optical micrograph of a detail of the previous specimen (x100)

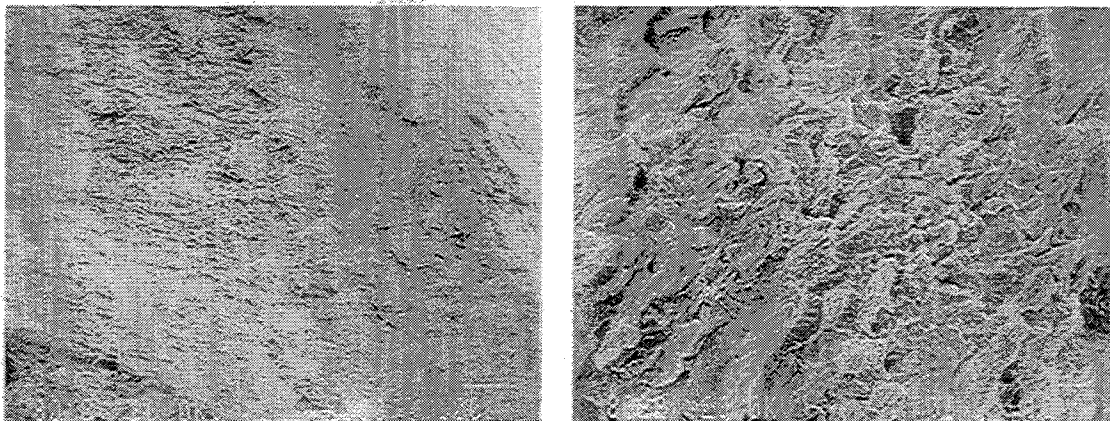


Figure 13: SEM micrographs of the fracture surface of a TStE355 steel specimen tested in granitic water at a strain rate of 10^{-7}s^{-1} and 90°C